

Variation of effective absorption bandwidth as a function of oblique angle for Cu, Co, and Ti co-doped SrFe₁₂O₁₉

Sự thay đổi của băng thông hấp thụ hiệu quả như là một hàm của góc xiên đối với SrFe₁₂O₁₉ đồng pha tạp Cu, Co, và Ti

Huynh Ngoc Toan^{a,b}, Tran Nguyen Tien^{a,b}, Tran Ngo^{a,b*}
Huỳnh Ngọc Toàn^{a,b}, Trần Nguyễn Tiến^{a,b}, Trần Ngô^{a,b*}

^aInstitute of Research and Development, Duy Tan University, 550000, Danang, Vietnam

^aViện Nghiên cứu và Phát triển Công nghệ cao, Trường Đại học Duy Tân, Đà Nẵng, Việt Nam

^bFaculty of Environmental and Natural Sciences, Duy Tan University, 550000, Danang, Vietnam

^bKhoa Môi trường và Khoa học Tự nhiên, Trường Đại học Duy Tân, Đà Nẵng, Việt Nam

(Ngày nhận bài: 31/01/2023, ngày phản biện xong: 11/3/2023, ngày chấp nhận đăng: 19/3/2023)

Abstract

Microwave absorbing materials (MAMs) are essential materials for mitigating the bad effects of electromagnetic interference and microwave pollution. SrFe_{12-2x}Cu_{x/2}Co_{x/2}Ti_xO₁₉ samples showed their superior microwave absorption performances in both reflection loss and effective absorption bandwidth (EAB) values for the normal incident angle of the microwave. Between these parameters, EAB values expressed how large a frequency the MAM could be used for practical applications. Most of the time, the EAB values would decrease with the increase of the incident angle, as shown in the $x = 0.05$ (M5) and $x = 0.10$ (M10) samples for transverse electric (TE) polarization mode, as well as the $x = 0$ (M0) and $x = 0.15$ (M15) samples for transverse magnetic (TM) polarization mode. Interestingly, the EAB values of the M0 sample increased from 10.87 GHz to a maximum value of 11.65 GHz at the incident angle of 29° for TE polarization mode. Similarly, the EAB values of the M15 sample were slightly increased from 9.79 GHz to the maximum value of 10.06 GHz at the incident angle of 30°. In the case of TM polarization mode, the M5 sample could maintain the EAB values in the incident angle range of 0–14°, while the EAB values of the M10 sample increased from 15.9 to 16.0 GHz when the incident angle reached 9°. The increase or maintenance of the EAB values could be attributed to the excellent values of complex permittivity and complex permeability as well as the matching between them. These results also proved that SrFe_{12-2x}Cu_{x/2}Co_{x/2}Ti_xO₁₉ samples could also be used as promising MAMs with a microwave incident angle of up to 70°.

Keywords: Hexaferrite; transition metal doping; microwave absorption; reflection loss; effective absorption bandwidth; oblique incident angle.

Tóm tắt

Vật liệu hấp thụ vi sóng là những vật liệu thiết yếu để giảm thiểu tác động của nhiễu điện từ và ô nhiễm vi sóng. Vật liệu SrFe_{12-2x}Cu_{x/2}Co_{x/2}Ti_xO₁₉ đã cho thấy hiệu suất hấp thụ vi sóng vượt trội của chúng ở cả giá trị suy hao phản xạ và băng thông hấp thụ hiệu quả (EAB) đối với góc tới bình thường của vi sóng. Trong hai thông số này, giá trị EAB thể hiện mức độ lớn vùng tần số mà vật liệu hấp thụ vi sóng có thể được sử dụng cho các ứng dụng thực tế. Thông thường, các giá trị EAB sẽ giảm khi tăng góc tới, được thể hiện trong các mẫu $x = 0,05$ (M5) và $x = 0,10$ (M10) đối với chế độ

*Corresponding Author: Tran Ngo, Institute of Research and Development, Duy Tan University, 550000, Danang, Vietnam; Faculty of Environmental and Natural Sciences, Duy Tan University, 550000, Danang, Vietnam

Email: tranngo@duytan.edu.vn

phân cực điện ngang (TE) và các mẫu $x = 0$ (M0) và $x = 0,15$ (M15) cho chế độ phân cực từ tính ngang (TM). Tuy nhiên, các giá trị EAB của mẫu M0 đã tăng từ 10,87 GHz lên giá trị tối đa là 11,65 GHz ở góc tới 29° đối với chế độ phân cực TE. Tương tự, giá trị EAB của mẫu M15 tăng nhẹ từ 9,79 GHz lên giá trị tối đa 10,06 GHz ở góc tới 30° . Trong trường hợp chế độ phân cực TM, mẫu M5 có thể duy trì các giá trị EAB trong phạm vi góc tới là $0-14^\circ$. Trong khi, giá trị EAB của mẫu M10 tăng từ 15,9 lên 16,0 GHz khi góc tới đạt 9° . Việc tăng/duy trì các giá trị EAB có thể được quy cho các giá trị tốt của độ từ thẩm phức và độ điện thẩm phức cũng như sự phù hợp giữa chúng. Những kết quả này cũng chứng minh rằng các mẫu $\text{SrFe}_{12-2x}\text{Cu}_{x/2}\text{Co}_{x/2}\text{Ti}_x\text{O}_{19}$ cũng có thể được sử dụng làm vật liệu hấp thụ vi sóng đầy hứa hẹn với góc tới vi sóng lên tới 70° .

Từ khóa: Hexaferrit; pha tạp kim loại chuyển tiếp; hấp thụ vi sóng; suy hao phản xạ; băng thông hấp thụ hiệu quả; góc tới xiên.

1. Introduction

Recently, wireless communication has become the most dominant communication method over traditional ones. Besides its advantages and convenience, this communication method also generates a new kind of pollution called electromagnetic (EM) radiation pollution [1-3]. To mitigate the effects of EM radiation pollution, one needs to consider electromagnetic interference (EMI) shielding. And fabricating microwave absorbing materials (MAMs) is one of the effective attempts at EMI shielding. To be considered effective MAMs, their properties should be as follows: intense reflection loss (RL), wide effective absorption bandwidth (EAB), thin, and lightweight.

Strontium M-type hexaferrite ($\text{SrFe}_{12}\text{O}_{19}$) could be considered a promising MAM due to its superior properties of high saturation magnetization (M_s), large coercive field (H_c), high magnetic uniaxial anisotropy, high Curie temperature (T_C), good chemical stability, an eco-friendly nature, and low cost [4-7]. However, it could only be applied in the several ten GHz frequency ranges due to its large magnetocrystalline anisotropy field (H_a), resulting in a high natural ferromagnetic resonance frequency (f_{FMR}) [8]. To reduce f_{FMR} to the frequency range of 2–18 GHz for daily applications, Cu, Co, and Ti elements were co-doped to $\text{SrFe}_{12}\text{O}_{19}$ with the composition of $\text{SrFe}_{12-2x}\text{Cu}_{x/2}\text{Co}_{x/2}\text{Ti}_x\text{O}_{19}$ where $x = 0, 0.05, 0.10, \text{ and } 0.15$, which were reported in our

previous work [9]. These samples showed excellent microwave absorption properties in both RL and EAB values. In the case of RL, all samples showed RL values of about -40 dB with the thickness varying in the range of 0.5–1.0 mm, meaning 99.99% of the incident microwave was absorbed by these samples with a very thin thickness. These samples also reached ultra-wide EAB values of about 10 GHz. Especially, the $x = 0.10$ sample could reach the EAB value of 15.9 GHz, which mostly covered the whole measured frequency range. It is worth noticing that these values were obtained for an incident angle of zero. However, the incident angle would vary from 0° to 90° in practical applications.

To investigate how the incident angle of microwaves affects the microwave absorption properties of $\text{SrFe}_{12-2x}\text{Cu}_{x/2}\text{Co}_{x/2}\text{Ti}_x\text{O}_{19}$ samples, the RL curves with the different microwave incident angles were carefully simulated for two different polarization modes: transverse electric (TE) and transverse magnetic (TM).

2. Experimental details

Cu, Co, and Ti co-doped $\text{SrFe}_{12}\text{O}_{19}$ samples were fabricated from high-purity (above 99.9%) Sigma-Aldrich chemicals of SrCO_3 , Fe_2O_3 , CuO , Co_3O_4 , and TiO_2 using ball milling combined with heat treatment. Precursors were weighed with nomination compounds of $\text{SrFe}_{12-2x}\text{Cu}_{x/2}\text{Co}_{x/2}\text{Ti}_x\text{O}_{19}$, with $x = 0, 0.05, 0.10, \text{ and } 0.15$ (named M0, M5, M10, and M15), then mixed by a Retsch MM200 miller for 1 h. After that, the powders were

pressed into button-shaped samples and sintered at 1000°C for 10 h. The samples were crushed using an agate mortar and pestle, re-milled for 1 h, and finally sintered at 1000°C for 12 h.

The microwave absorption properties of the samples were investigated through S-parameter (S_{11} , S_{21} , S_{12} , and S_{22}) measurements using a vector network analyzer (VNA, Keysight PNA-X N5242A). Before investigating S-parameters, the samples were mixed with paraffin for a volume ratio of 4:6. After that, the paraffined powders were molded into toroidal-shaped devices with inner and outer diameters of 3.04 and 7.00 mm using a special mold. The complex permittivity and complex permeability data were extracted from S-parameter data using the Nicolson-Ross-Weir (NRW) method. Then, the microwave absorption properties of paraffined samples were accessed through reflection loss (RL) values as a function of frequency and thickness. RL values were calculated using transmission line theory. Finally, the thickness showed the best EAB for each sample with the normal incident angle used for the oblique angle investigation.

3. Results and discussion

Based on our previous report, the thicknesses for the best EAB values for M0, M5, M10, and M15 samples with the normal incident were 1.25, 0.75, 1.25, and 1.50 mm, respectively [9]. Therefore, these thicknesses were selected for the study of microwave absorption properties as a function of incident angle using transmission line theory in the case of an oblique incident. In addition, the study on the effects of oblique incidents on microwave absorption performance was beneficial for practical applications. This investigation would be conducted for two different polarization modes, TE and TM.

The RL in the case of an oblique angle could also be calculated using transmission line theory with the following equation:

$$RL = -20 \log |\Gamma|, \tag{1}$$

where Γ is the symbol of the reflection coefficient, which has two modes of TE and TM. The Γ value of each mode could be calculated from input impedance (Z_{in}), free space impedance (Z_0), and incident angle (θ) by the following equations:

$$\Gamma(\text{TE}) = \frac{Z_{in} - Z_0 / \cos \theta}{Z_{in} + Z_0 / \cos \theta}, \tag{2}$$

$$\Gamma(\text{TM}) = \frac{Z_{in} - Z_0 \cos \theta}{Z_{in} + Z_0 \cos \theta}. \tag{3}$$

Based on Snell's law, the relationship between θ and the angle of refraction φ is as follows:

$$\cos \varphi = \sqrt{1 - \frac{\sin^2 \theta}{\mu_r \epsilon_r}}. \tag{4}$$

Based on transmission line theory, Z_{in} of two polarization modes could be expressed as:

$$Z_{in}(\text{TE}) = \frac{Z_0 \sqrt{\mu_r / \epsilon_r}}{\cos \varphi}, \tag{5}$$

$$Z_{in}(\text{TM}) = Z_0 \sqrt{\mu_r / \epsilon_r} \cos \varphi, \tag{6}$$

Following that, the impedance in the case of an oblique angle (Z_{in_obl}) could be calculated as:

$$Z_{in_obl} = Z_{in} \tanh(vd), \tag{7}$$

$$v = j \frac{2\pi}{\lambda_0} \sqrt{\mu_r \epsilon_r} \cos \varphi, \tag{8}$$

where v is the propagation constant and λ_0 stands for wavelength in free space.

Figure 1 shows the three-dimensional (3D) RL images for optimal thickness for each composite in the TE polarization mode in the frequency and angle ranges of 2–18 GHz and 0–89°, respectively. In each 3D RL image, the black and red curves denote the effective absorption areas (EAAs) of -10 and -20 dB, respectively, meaning 90% and 99% of the

incident microwave was absorbed by the composites. In all cases, 90% of the incident microwave was absorbed (named the effective absorption rate) for an incident angle varying in

the range of 0–60°. However, these values could not be observed for the whole measured frequency range.

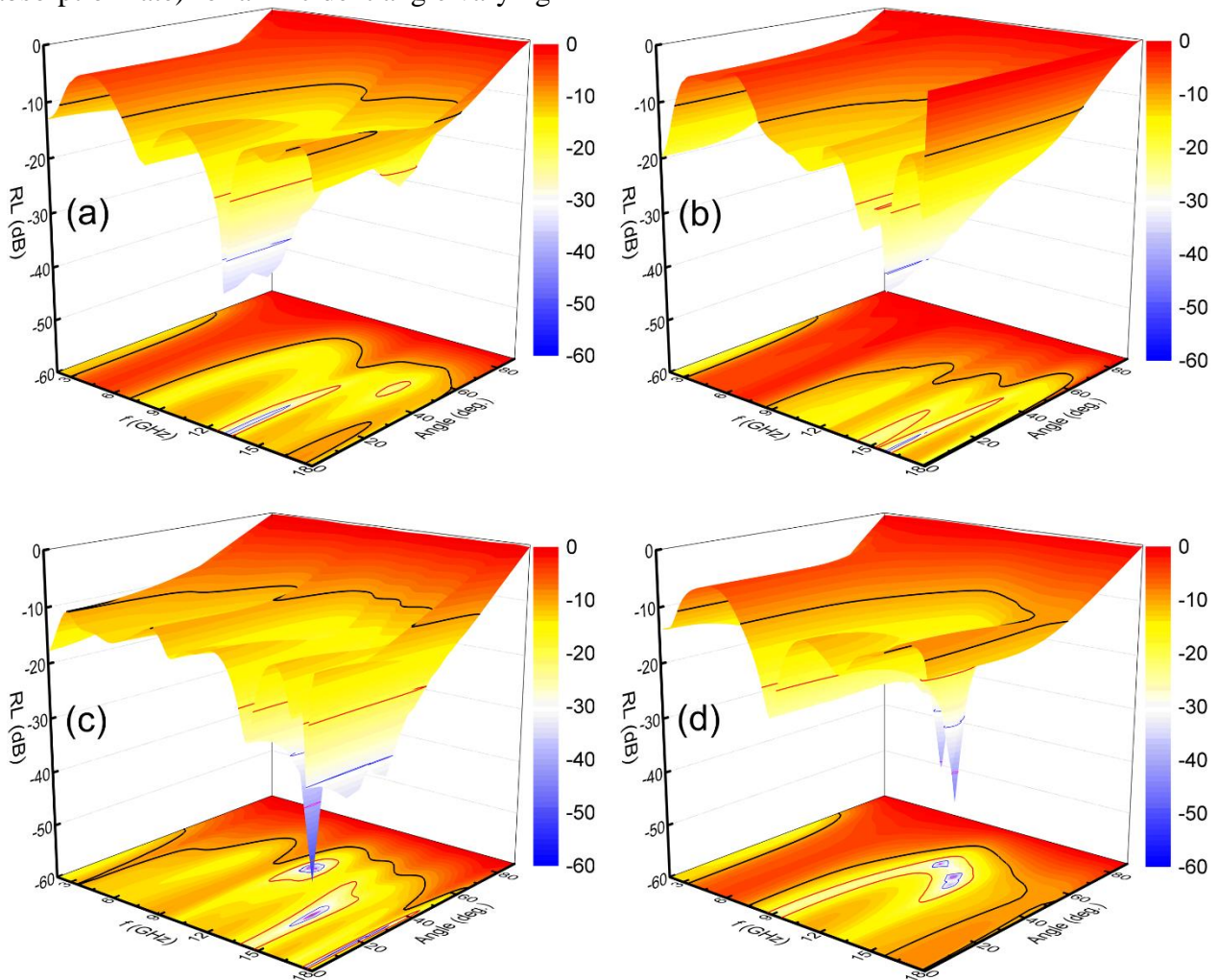


Figure 1. 3D RL images for TE polarization mode at different frequencies and angles of incidence for optimum thicknesses of (a) M0, (b) M5, (c) M10, and (d) M15 paraffined samples.

To have a specific observation on the variations of RL values as a function of frequency and angle, the contour RL maps for all composites were plotted and shown in **Fig. 2**. For the M0 composite, there were two EAAs over the frequency ranges of 2–3 GHz and 7–18 GHz, as shown in **Fig. 2(a)**. In the first area, the effective absorption rate (EAR) could be maintained up to more than 60°. While the second area could maintain the EAR up to about 70°. However, there was a low EAA inside the second area in the range of 16.5–17.0 GHz. The M5 composite also had two EAAs,

as shown in **Fig. 2(b)**. The first area was similar to that of the M0 composite. While the second area was smaller than that of the M0 composite. Some areas could absorb 99% and 99.9% of the incident microwave, which was denoted by red and blue curves, respectively. These areas were located in the high-frequency and low-incidence angle ranges. The microwave absorption properties for the case of TE polarization mode reached their best in the case of the M10 composite, where the first and second EAAs tended to collapse, leading to the largest EAA, as shown in **Fig. 2(c)**. The

number and area of red and blue areas were also better than those of M0 and M5 composites. The EAAs were narrowest in the case of the M15 composite, where the second EAA was much smaller than those of the M0–10 composites, as shown in **Fig. 2(d)**. However, the red area with an EAR of 99% for M15 composite was the largest compared to those of M0–10 composites. At the normal incident, the maximum EAB values of M0–M15 composites were 10.87, 10.27, 15.90, and 9.79 GHz, respectively. With the increase in incident angle, the EAB value of the M0 composite increased to its maximum value of 11.65 GHz

at an incident angle of 29°. After that, the EAB values decreased with the increase in incident angle and reached zero when the incident angle passed 70°. Note that the EAB value at 50° of incident angle was similar to that at 0°. Similarly, the EAB values of M15 samples were slightly increased with the increase in incident angle and reached a maximum of 10.06 GHz at 30° and slightly decreased after that. The EAB values of the M5 and M10 samples gradually decreased with the increase in incident angle and also reached zero when the incident angle passed the value of 70°.

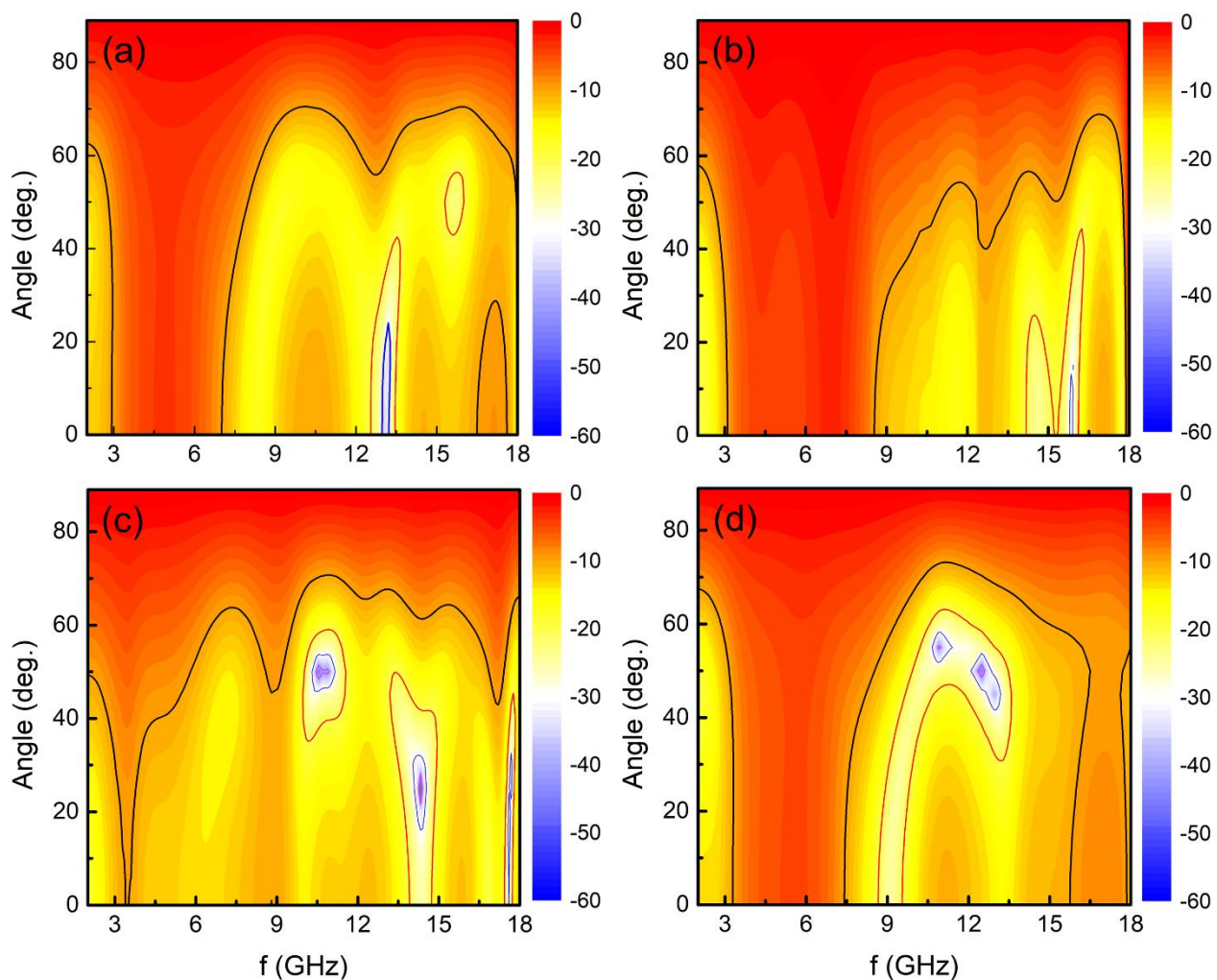


Figure 2. RL contour maps for TE polarization mode at different frequencies and angles of incidence for optimum thicknesses of (a) M0, (b) M5, (c) M10, and (d) M15 paraffined samples.

Figure 3 shows the 3D RL images for TM polarization mode with the same optimal

thickness as well as frequency and incident angle ranges as those in **Fig. 1**. In each 3D

image, some areas are marked by black, red, and blue curves, which correspond to areas with microwave absorption rates of 90%, 99%, and 99.9%, respectively. In general, M0 and M15 composites showed poor microwave

absorption properties with narrow EAAs, as shown in **Fig. 3** (a, c). While M5 and M10 composites revealed better microwave absorption properties with much larger EAAs, as shown in **Fig. 3**(b, d).

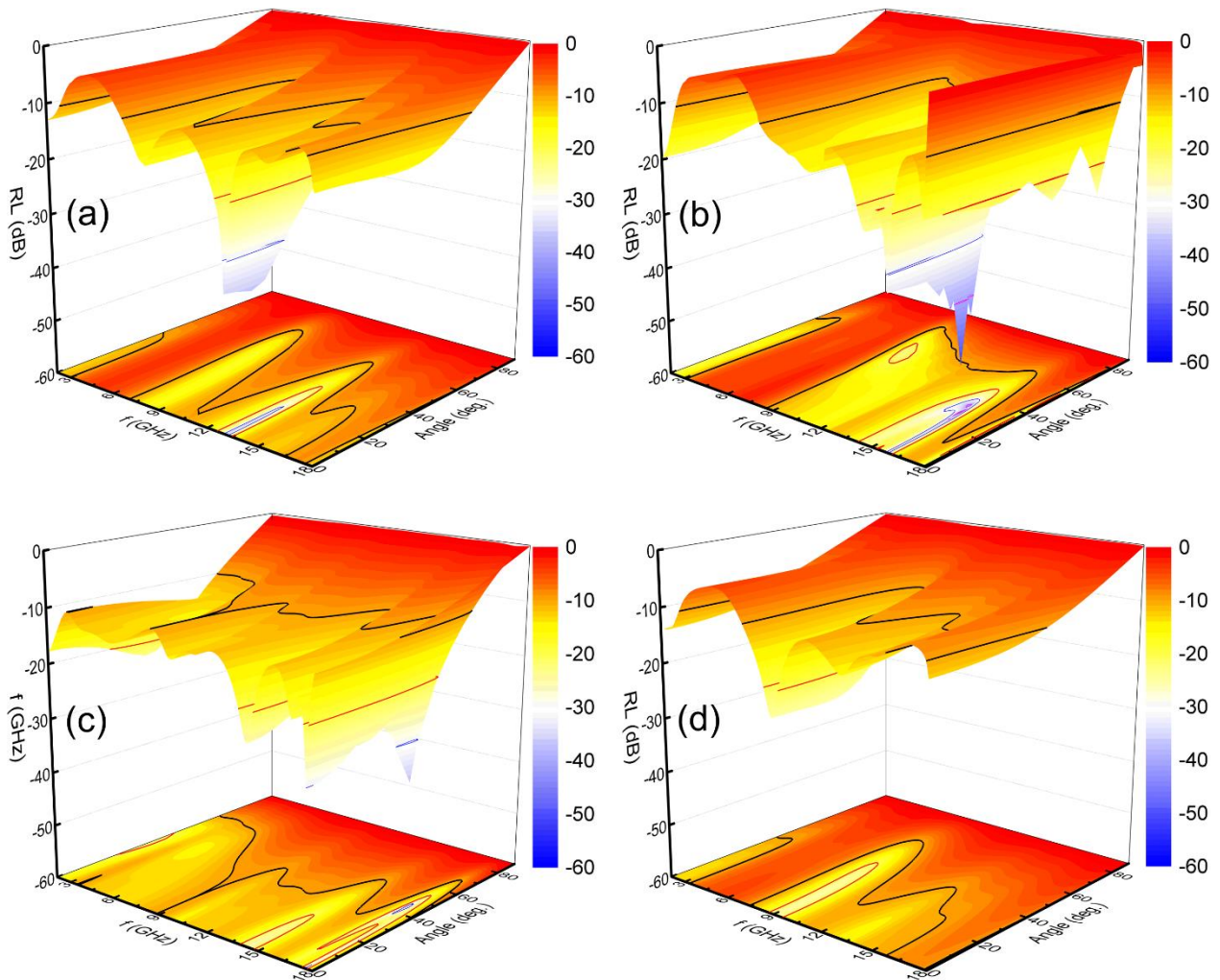


Figure 3. 3D RL images for TM polarization mode at different frequencies and angles of incidence for optimum thicknesses of (a) M0, (b) M5, (c) M10, and (d) M15 paraffined samples.

To compare the microwave absorption properties of composites with the variation of frequency and incident angle in the case of TM mode, RL contours for all composites were plotted and shown in **Fig. 4**. Three regions could absorb more than 90% of the incident microwave for M0 composites: two tiny EAAs were at the two ends of the measured range, and the main EAA was located in the frequency range of 7–6.5 GHz, as shown in **Fig. 4**(a). This main area could be maintained in the EAR up

to 70° at some specific frequency, such as 7.5 GHz. In addition, this main area also contained some areas that could absorb more than 99% of the incident microwave, as denoted by the red curve in **Fig. 4**(a). The microwave absorption properties were enhanced for the composites with higher doping concentrations. The EAAs of the M5 composite were larger than those of the M0 composite, as shown in **Fig. 4**(b). The EAR could be maintained up to 80° at a frequency of 9 GHz, and the 99% absorption

rate areas were extended. The microwave absorption properties were excellent for the M10 composite, where the composite could absorb 90% of the incident microwave in the whole measured frequency range, as shown in **Fig. 4(c)**. Therefore, the maximum EAB value of the M10 composite was 16 GHz. In addition, the EAAs were also the largest compared to other composites. With higher doping concentrations, the microwave absorption properties were poor in both EAAs and EARs, as shown in **Fig. 4(d)**.

As mentioned above, the maximum EAB values of M0–M15 samples were 10.87, 10.27,

15.90, and 9.79 GHz, respectively. In the case of TM polarization mode, the EAB values of M0 and M15 composites decreased with the increase of the incident angle, and these composites would have no EABs when the incident angles were about 70°. On the contrary, the EAB values of the M10 composite slightly increased with the increase of incident angle and reached maximum EAB values of 16 GHz (covering the whole measured range) at an incident angle of 9°. For the M5 composite, the EAB values were mostly maintained as constant when the incident angle increased from 0° to 14° and slightly increased after that.

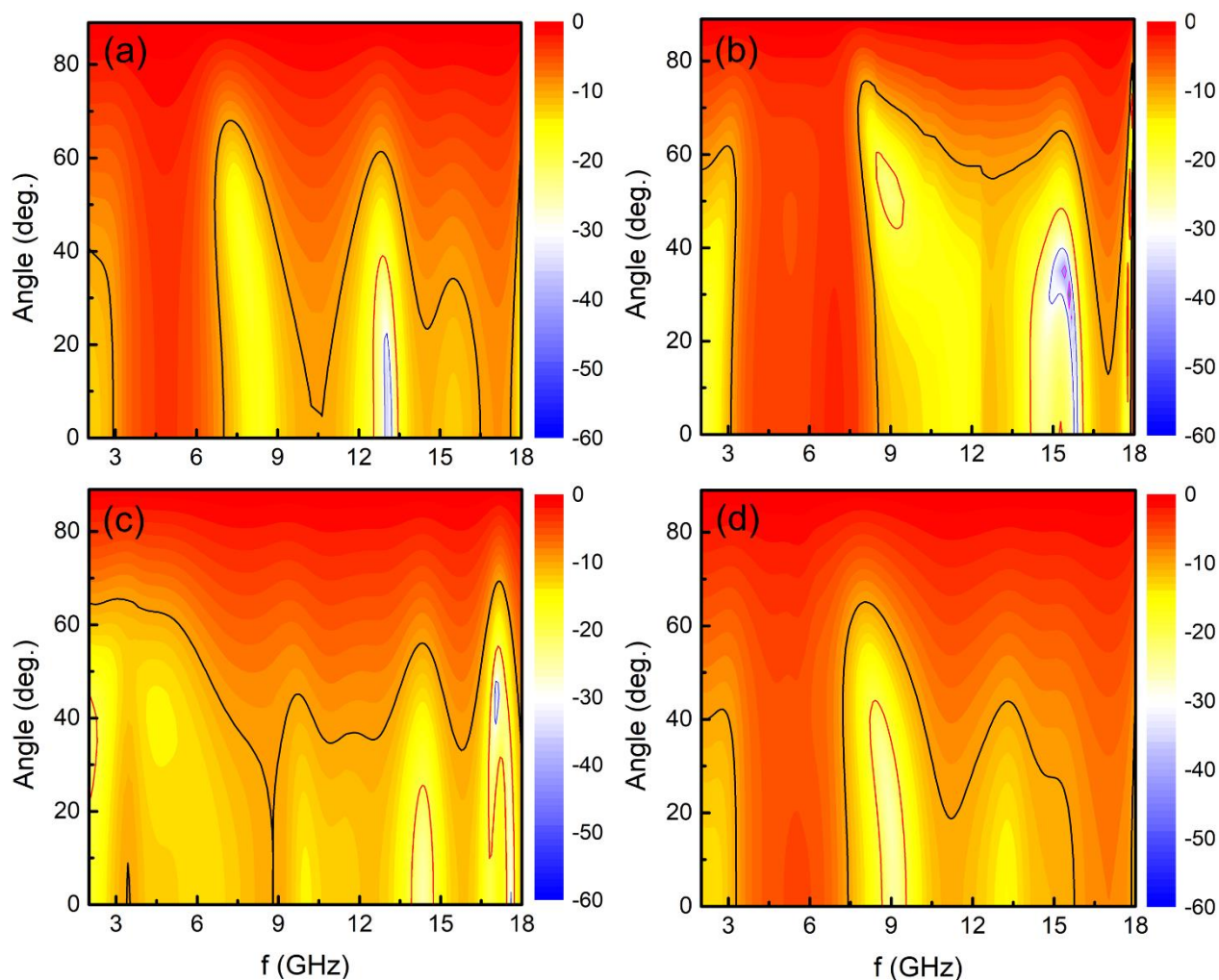


Figure 4. RL contour maps for TM polarization mode at different frequencies and angles of incidence for optimum thicknesses of (a) M0, (b) M5, (c) M10, and (d) M15 paraffined samples.

The good microwave absorption properties of the M10 composite compared to those of

other composites could be a result of its excellent values of complex permittivity and

complex permeability, as well as the matching between them [10]. Besides, the microwave incident and refraction angles could also be used to explain the excellent microwave absorption performance [11-13]. When the microwaves hit the composites and then propagated into them, there would be an occurrence of refraction. Based on Eq. (4), a small refraction angle is a result of the high value of the product of μ_r and ϵ_r . Therefore, there was almost no refraction angle for the small incident angle [14], resulting in almost the same RL values as the normal case (the incident angle is zero). With much larger incident angles, the propagation pathway of the incident microwave in the composites was longer and even passed the value of a quarter wavelength, resulting in the decrease of RL values due to the impedance mismatch [13]. When the incident angle gets close to the highest value of 90° , the RL values tend to be zero because the incident microwave is only reflected at the interfaces of the composites and air.

4. Conclusion

In this work, the effects of incident angle on the microwave absorption properties of the composites of Cu, Co, and Ti co-doped $\text{SrFe}_{12}\text{O}_{19}$ samples with paraffin were fully investigated in TE and TM polarization modes. The work revealed that the good microwave absorption properties (especially in the case of EAB values) of the composites maintained their good values when the microwave incident angle increased from 0 to 50° for both TE and TM polarization modes. With a larger incident angle, there were still values of EAB up to $\sim 70^\circ$, but they vanished when the incident angle tended to 90° . Interestingly, the EAB values of composites were even enhanced with the increased incident angle. In the undoped (M0) composite in the case of TE polarization mode, the EAB reached the maximum value of

11.65 GHz at the incident angle of 29° , which was higher than the EAB value of the normal incident angle of 10.87 GHz. M15 composite also showed an enhancement in EAB value with a value of 10.06 GHz at 30° , which was larger than the EAB value of 0° . In the case of the TM polarization method, only the M10 composite showed an enhancement in EAB values from 15.9 to 16 GHz. These increases in EAB values could be attributed to their excellent values of complex permittivity, and complex permeability, as well as their matching.

Acknowledgment

The authors sincerely thank Duy Tan University for creating the conditions and facilities to complete this study. This research belongs to the grassroots-level topic code Đ21-22 KT1-2 for the academic year 2022–2023.

References

- [1] A.A. Al-Ghamdi, O.A. Al-Hartomy, F.R. Al-Solamy, N. Dishovsky, P. Malinova, G. Atanasova, N. Atanasov. (2016). Conductive carbon black/magnetite hybrid fillers in microwave absorbing composites based on natural rubber. *Compos. B. Eng.*, *96*, 231-241. <https://doi.org/10.1016/j.compositesb.2016.04.039>.
- [2] L. Huang, X. Liu, R. Yu. (2018). An Efficient Co/C Microwave Absorber with Tunable Co Nanoparticles Derived from a ZnCo Bimetallic Zeolitic Imidazolate Framework. *Part. Part. Syst. Charact.*, *35*, 1800107. <https://doi.org/10.1002/ppsc.201800107>.
- [3] H.B. Baskey, S.K. Singh, M.J. Akhtar, K.K. Kar. (2017). Investigation on the Dielectric Properties of Exfoliated Graphite-Silicon Carbide Nanocomposites and Their Absorbing Capability for the Microwave Radiation. *IEEE Trans. Nanotechnol.*, *16*, 453-461. [10.1109/TNANO.2017.2682121](https://doi.org/10.1109/TNANO.2017.2682121).
- [4] M.A. Almessiere, Y. Slimani, S. Guner, S. Aldakhil, A.D. Korkmaz, M. Sertkol, H. Gungunes, G. Yasin, A. Baykal. (2020). Ultrasonic synthesis, magnetic and optical characterization of Tm^{3+} and Tb^{3+} ions co-doped barium nanohexaferrites. *J. Solid State Chem.*, *286*, 121310. <https://doi.org/10.1016/j.jssc.2020.121310>.
- [5] J.R. Liu, R.Y. Hong, W.G. Feng, D. Badami, Y.Q. Wang. (2014). Large-scale production of strontium

- ferrite by molten-salt-assisted coprecipitation. *Powder Technol.*, 262, 142-149. <https://doi.org/10.1016/j.powtec.2014.04.076>.
- [6] Q. Wu, Z. Yu, Y. Wu, Z. Gao, H. Xie. (2018). The magnetic and photocatalytic properties of nanocomposites SrFe₁₂O₁₉/ZnFe₂O₄. *J. Magn. Magn. Mater.*, 465, 1-8. <https://doi.org/10.1016/j.jmmm.2018.05.098>.
- [7] J.-P. Lim, M.-G. Kang, Y.-M. Kang, Development of Multi-Cation-Doped M-Type Hexaferrite Permanent Magnets, *Appl. Sci.*, 2023.
- [8] K.A. Korolev, S. Chen, R. Barua, M.N. Afsar, Y. Chen, V.G. Harris. (2016). Millimeter wave transmittance/absorption measurements on micro and nano hexaferrites. *AIP Adv.*, 7, 056101. 10.1063/1.4973597.
- [9] P.T. Tho, C.T.A. Xuan, N. Tran, N.Q. Tuan, W.H. Jeong, S.W. Kim, T.Q. Dat, V.D. Nguyen, T.N. Bach, T.D. Thanh, D.T. Khan, B.W. Lee. (2022). Ultra-wide effective absorption bandwidth of Cu, Co, and Ti co-doped SrFe₁₂O₁₉ hexaferrite. *Ceram. Int.*, 48, 27409-27419. <https://doi.org/10.1016/j.ceramint.2022.05.389>.
- [10] J. Zhang, P. Wang, Y. Chen, G. Wang, D. Wang, L. Qiao, T. Wang, F. Li. (2018). Microwave Absorption Properties of Co@C Nanofiber Composite for Normal and Oblique Incidence. *J. Electron. Mater.*, 47, 4703-4709. 10.1007/s11664-018-6351-1.
- [11] J. Feng, Y. Zhang, P. Wang, H. Fan. (2016). Oblique incidence performance of radar absorbing honeycombs. *Compos. B. Eng.*, 99, 465-471. <https://doi.org/10.1016/j.compositesb.2016.06.053>.
- [12] J.-W. Kim, S.-S. Kim. (2010). Microwave absorbers of two-layer composites laminate for wide oblique incidence angles. *Mater. Des.*, 31, 1547-1552. <https://doi.org/10.1016/j.matdes.2009.09.054>.
- [13] L. Zhang, H. Lu, P. Zhou, J. Xie, L. Deng. (2015). Oblique Incidence Performance of Microwave Absorbers Based on Magnetic Polymer Composites. *IEEE Trans. Magn.*, 51, 1-4. 10.1109/TMAG.2015.2439682.
- [14] S. Kim. (2011). Microwave Absorbing Properties of Magnetic Composite Sheets for Oblique Incidence Angles. *IEEE Trans. Magn.*, 47, 4314-4317. 10.1109/TMAG.2011.2157465.